DECEMBER 1983 LRP 231/83

MHD-LIMITS TO PLASMA CONFINEMENT

F. Troyon, R. Gruber, H. Saurenmann,

S. Semenzato, S. Succi

Invited Paper presented by F. Troyon to the XI European Conference on Controlled Fusion and Plasma Physics, Aachan, September 1983

MHD-LIMITS TO PLASMA CONFINEMENT

F. Troyon, R. Gruber, H. Saurenmann, S. Semenzato, S. Succi

Centre de Recherches en Physique des Plasmas
Association Euratom - Confédération Suisse
Ecole Polytechnique Fédérale de Lausanne
21, Av. des Bains, CH-1007 Lausanne/Switzerland

ABSTRACT

Ideal MHD restricts both the current and the pressure which can be stably confined in a Tokamak. A pressure profile optimisation is carried out for a variety of equilibria, which include JET and INTOR-like plasmas, in order to obtain the maximum β which can be stably confined at constant current. The current is limited to a value corresponding to a safety factor slightly above 2 at the plasma surface. A simple scaling law is found that fits well all the cases and which predicts a linear rise of β with the current.

I. INTRODUCTION

With the large amount of power now available on many Tokamak experiments, the existence of a β limit is no longer only a subject of theoretical speculation. It is also an experimental fact and a source of worry for the large expriments now coming into operation and for the future of the whole Tokamak line. The onset of ideal MHD instabilities growing on the fast Alfvén time scale of the order of microseconds could provide such a limit. Resistivity will undoubtly lead to instabilities before the ideal limit is reached, making maybe such a limit soft, but the parametric dependence of the ideal limit on geometry and physical parameters, such as current and pressure, should then be reflected in the dependence of the level of turbulence, of the amplitude of relaxation oscillations, of the size of the deformation or of the sensitivity to disruptions on these parameters. It might also manifest itself only as a hard disruptive limit with no precursor sign, analogously to the axisymmetric instability.

This paper presents a summary of studies carried out specifically for JET and INTOR, with some additional material on the influence of the plasma shape and aspect ratio. Also a critical examination of the limitations inherent in calculations, such as those in which classes of profiles with a few parameters are chosen for the optimisation, has been made in order to try to extract conclusions as general as possible.

II. PLASMA SHAPES, CURRENT AND PRESSURE PROFILES

The shape of the plasma surface is given, in cylindrical coordinates, r, z, ϕ centered on the axis of the torus, by the parametric expressions

$$r = R + a\cos(\Theta + \gamma\sin\Theta)$$

$$z = Ea\sin\Theta, \qquad (1)$$

where R is the major radius, a the horizontal half-width of the plasma, E the elongation and γ the triangularity. INTOR is defined by the set of parameters: $R/a = 4$, $E = 1.6$, $\gamma = 0.3$, while the set $R/a = 2.36$, $E = 1.68$, $\gamma = 0.3$, well represents the JET shape. The equilibrium requires specification of 2 source terms, which can be the pressure gradient $dp/d\psi$ and the toroidal flux function $T \equiv rB_\phi$. We have chosen polynomial expressions for these two arbitrary functions:

$$T^2(\psi) = T^2_{vac} + t\psi^2$$
$$p(\psi) = p_1\psi^2 + p_2\psi^3,$$

where ψ is the usual flux function with $\psi_s = 0$ at the plasma surface and $\psi_0 < 0$ at the magnetic axis and where p_1, p_2, and t are 3 free parameters. The indices o and s always refer to the magnetic axis and the plasma surface, respectively. With the three parameters p_1, p_2 and t, we can vary the total current I, the safety factor on axis q_o and the poloidal $\beta_J \equiv 8\pi\int pds/\mu_o I^2$.

III. STABILITY OF "INTOR-LIKE PLASMAS"

By "INTOR-like" plasmas we mean any plasma of aspect ratio 4 having a surface as defined by eq. 1. INTOR itself has a major radius of 5.2 m and a T_S of 286 Tm. The stability of INTOR equilibria is investigated numerically with ERATO (Gruber et al., 1981 a), keeping the current I fixed and varying the two remaining parameters q_0 and $\beta \equiv 2\int pdV/\int B^2 dV$ (an alternative choice to β_J) with no conducting shell around the plasma. Figure 1 shows the results for a series of ascending currents, from 4.7 MA to 9.4 MA. The limits shown on each diagram are the ballooning limit B, the Mercier limit on axis M and the n = 1 free boundary kink-limit. The n = 1 limit is to be understood as a σ-stability limit (Goedbloed and Sakanaka, 1974). In the ERATO code the truncation error associated with the discretisation leads, for Tokamak profiles, to a destabilisation of the spectrum. Whenever there is a singular surface within the plasma, the continuous spectrum extends to the marginal point. The discretisation destabilizes the marginal mode and a convergence study to zero mesh size is needed to verify that it is indeed marginal. We have found that for these equilibria, the destabilisation of the marginal mode, measured by the negative contribution $\Delta\omega^2$ to the eigenvalue, normalized to the Alfvén transit frequency across the major radius calculated with the field on axis and a constant density, is of the order of 10^{-4} for a 60 x 60 mesh. Rather than doing costly convergence studies for each point, we have taken the value of the square of the normalized growthrate of 10^{-4} as the stability limit. In addition, by looking at the mode structure we can recognize the destabilized marginally stable modes which belong to the lower edge of the continuum.

The n = 1 kink limit above q_0 = 1 truly appears as a β limit, although the allowed range of q_0 shrinks as q_S = 3 is crossed at a current of about 7.1 MA. This limit appears to be a hard one as the growthrate increases rapidely when it is crossed. A series of equilibria which all lie on the n = 1 limit for I = 5.9 MA is shown in fig. 2. The q profile does not seem to be a critical parameter at this current. Figure 3 shows the poloidal flow associated with an unstable mode which develops when β exceeds the limit. The parameters for this case are q0 = 1.35, β = 3 % and I = 5.9 MA, corresponding to a β which lies about 1 % above the stability limit. The mode is global and the normalized growthrate is 0.1, corresponding typically to a growthtime of a few microseconds for INTOR. Below q_o = 1, the poloidal flow looks like an internal kink with strong activity on the q = 2 and q = 3 surfaces and near the plasma surface. The limit at $q_o < 1$ is soft and, since internal kinks are weakly growing with normalized growthrates squared of around 10^{-4} or even lower, to take 10^{-4} as the stability limit is probably optimistic. This is unimportant as long as the Mercier criterion provides a higher limit on q_o.

When the ballooning limit B is crossed, an unstable ballooning region appears between the axis and the surface, between 0.5 and 0.8 of the total flux. The region below B is in the first region of stability. Since on the magnetic axis, both Mercier and the ballooning criterion coincide, there must be also an unstable ballooning region near the axis. But near the axis there is little modulation of the equilibrium quantities and it becomes very difficult to test the ballooning criterion because numerical discretisation errors become dominant. We assume that the ballooning limit for this region coincides with the Mercier limit on axis, since Mercier is most stringent there.

We have also looked at higher n free-boundary modes. For the case of I = 5.9 MA on which we have concentrated most of our effort we have determined the σ-stability limit for n = 2 and n = 4, with the same value of the normalized growthrate σ as for n = 1. In these two cases a conducting shell was placed at a distance 3a from the plasma in order to be able to work with a version of ERATO (Gruber et al., 1981 b) which improves the convergence for higher n modes. The result is shown in fig. 4, together with the n = 1 and B, M limits.

The higher n modes have less stringent requirements for stability than the n = 1 kink mode but the difference on the limiting β is insignificant. There does not seem to be any interest in wall stabilizing the low n modes. The rapidity with which higher n modes become unstable as the n = 1 stability limit is crossed is also an indication of the difficulty of trying to improve on this limit. Collecting the maximum stable values of β for each value of the current I from figure 1 (indicated by +) we see that this limiting β increases, to a good approximation, linearly with the current (Fig. 5). The small modulation around the straight line appears to be correlated with the crossing of integer q surfaces through the plasma surface; but the stability boundaries in fig. 1 have error bars due to the fact that a finite number of equilibria have been generated for each value of the current and interpolation had to be done to obtain the curves shown in fig. 1, so that the dispersion around the straight line may just be an indication of the accuracy of the optimisation.

The pressure, safety factor and q profiles of the equilibrium with I = 9.4 MA, q_0 = 1.26 and β = 3.7 % which have the highest stable β values are shown in fig. 6 (we did not find stable equilibria beyond I = 9.4), which corresponds to q_S = 2.2. The Mercier criterion prevents q_0 from dropping near the axis and, with more current in the plasma, q develops deeper minima off axis and Mercier and ballooning criteria become violated there. As usual for Tokamak profiles, when Mercier is violated, there is also a n = 1 free boundary instability. The necessity of keeping q_S above 2 to prevent the n = 1 instability has been seen in every parametric study published so far.

In order to gain some information on the effects of plasma shape we have varied E and γ in an unsystematic way, repeating each time the optimisation procedure. The β, q_0 stability diagrams have the same appearance in all cases. The results are also shown in fig. 5. Fewer equilibria have been used so that the results are not as dense, in the β,q_0 plane, as for the INTOR shape and the inaccuracy is thus larger than for these cases, although certainly not as large as suggested by the spread of the points around the linear INTOR fit. It is nevertheless surprising that the additional points cluster so close to a single straight line. It implies that for the same current, the limiting β is the same. But the maximum current which can be carried before the same difficulty arises as in INTOR when q_S drops below 2 depends on the configuration. But this maximum current increases with increasing elongation and triangularity so that higher β can effectively be obtained with higher triangularity and elongation.

IV. STABILITY OF JET

The optimisation has been repeated for the conditions of JET, in the so-called regime of extended performance, with T_S = 105 Tm and R = 2.96 m. The current planned for extended performance is 4.8 MA and the results are shown in fig. 7 for this current. The curves labeled with an asterisk are the stability limits with a shell tight against the plasma boundary while the others are with no shell. The same σ-limit as in INTOR has been taken in all cases.

All the comments made about the INTOR results apply to the JET case. The calculation has been repeated for different values of the current. Two stability limits are shown in fig. 8. The first (indicated by .) which is the limit obtained by considering the Mercier limit. It turns out to be also the optimum for stability to the n = 1 mode. The second limit, (indicated by Δ), which is more stringent than the first, is given by the requirement that all n be stable. The Δ for I = 4.8 MA corresponds to the intersection of the n = 1 and B limits in fig. 7. We have not verified in all cases that all intermediate n modes are indeed stable at this limit, assuming the behaviour shown in figs. 4 and 7 is general.

At high current the difference between the 2 limits becomes important in contrast to INTOR which has a larger aspect ratio. This difference reflects the limitation of the polynomial expression used. With more free parameters the pressure profile could be easily adjusted by a redistribution of the pressure gradient from the narrow ballooning unstable region to the rest of the plasma, thus pushing the ballooning limit up to the n = 1 kink limit. There is a maximum value for the current, corresponding again to q_S of the order of 2.3, beyond which we not longer find stability to kink and ballooning modes. We have not succeeded in following the drop of the stability limit from its maximum value. The profiles corresponding to the highest β fully stable equilibrium are shown in fig. 9. In Tokamaks, the violation of the Mercier criterium is always associated with global instabilities. This prevents q_0 from decreasing, not only on axis but also at the off-axis minima, and it seems there is no room for putting more current in the plasma. Already at 12 MA it is not possible with the profiles chosen to have full stability.

DISCUSSION OF THE RESULTS

The picture which emerges from these case studies is simple. The $n = 1$ free-boundary stability imposes a limit on β. The highest β is reached when q_0 is near the Mercier limit on axis, slightly above 1. This limiting β increases with the current until the q profile becomes flat over most of the plasma and q_s reaches about 2. Figure 10 shows that the results for JET, INTOR (standard case) and an intermediate case with an aspect ratio of 3 with the same shape as INTOR ($E = 1.6$, $\gamma = 0.3$) can be described by a single linear relationship between βA and $I_N \equiv \mu_0 I A^2/T_S$, where $A \equiv R/a$ is the aspect ratio:

$$(\beta A)_{max} \approx 2.2\ I_N.$$

For a given I, the INTOR results show a weak dependence, if any, of $\beta(I)$ on the plasma shape or elongation. The other points on the INTOR diagram (fig. 5) would also cluster around the same line, making the results even more surprising. If this law is extrapolated to a circular shape and large aspect ratio it can be rewritten as

$$\beta_{pmax} \approx 0.14\ Aq_s,$$

where q_s is the safety factor at the plasma surface. A relation of the same type has been frequently conjectured (Kerner et al., 1981), without the dependence on q_s, in the form $\beta_{pmax} \approx A/2$. The two limits coincide at $q_s \approx 3.5$.

Within the framework of ideal MHD and without introducing non linear saturation mechanisms or non-axisymmetric modifications to the equilibrium, there are 3 directions which could be pursued to improve the β limit: changes in the current and pressure profiles, and wall stabilisation.

At low current, as seen in figs 1 and 7, the current profile, which essentially controls the q profile, does not influence the $n = 1$ limit unless one reaches values of $q_0 < 1$. The current profile can only be of importance at the highest current. When q_s approaches 2, a drop of q_0 below 1 could lead to a gain in β, provided the Mercier-ballooning modes and the internal kink do not appear. Imposing that the pressure gradient vanishes in a region around the axis would remove all ballooning modes there and according to the results of Bussac et al. (1975), would also suppress the internal kink, at least for nearly circular cross-section and large aspect ratio plasmas. The ballooning criterion will limit this shift of the pressure gradient to the outer region where it is most dangerous. We do not have yet enough data to quote an estimate of the size of the improvement, if there is any.

The pressure profile is an important factor. It is precisely the introduction of the extra term p_2 in the expression (1) for the pressure gradient that has led to a large improvement over the β values quoted by Todd et al. (1979). The calculations reported in (Todd et al., 1979; Charlton et al., 1982; Bernard et al., 1980; Kerner et al., 1981) were all made by varying the current or q profiles and fixing the pressure gradient to be either proportional to the current or to have a simple analytic form. Optimisation of the pressure profile has only been done for the ballooning stability. It is probable that some improvement over the β limit quoted can still be achieved by proper tailoring of the profile, but we have not succeeded in identifying a specific feature of the pressure profile which has a definite influence on the $n = 1$ free boundary stability.

Wall stabilisation is a recipe to avoid low-n instabilities. But its effectiveness has to be assessed for each device so that it is not possible to draw general conclusions. For example, in the present conceptual design of INTOR, with its segmented structure, it is highly doubtful that even $n = 1$ could be wall stabilized. JET has a continuous wall which will be effective on the fast time scale. The example of the axisymmetric instability shows that passive stabilisation on the fast time scale does not imply long term stability. The RFP is an example which shows just the opposite behaviour, since it is MHD unstable without the wall and yet is stable on the slow time scale, but the poor confinement observed so far maybe an indication of the price to be paid for purely passive stabilisation.

ACKNOWLEDGEMENTS

During the course of this work we have benefited from helpful discussions with Dr. T. Stringer and his team at JET, with Dr. J. Wesson, who has already noted that some of the published results in Kerner et al. (1981) when crossplotted also indicated a linear dependence of β on the current, with Dr. F. Engelmann and the Garching Stability group.

This work has been carried out under the JET contract JB1/9018 and the NET/INTOR contract 087/81-12/FU-CH/NET. It is also supported by the Swiss National Science Foundation and the Federal Institute of Technology, Lausanne.

REFERENCES

1 Bernard, L.C., D. Dobrott, F.J. Helton, R.W. Moore, Nucl. Fusion 20 (1980) 1199.

2 Bussac, M.N., R. Pellat, D. Edery, J.L. Soulé, Phys. Rev. Letters 35 (1975), 1638.

3 Charlton, L.A., R.A. Dory, Y.K.M. Peng, D.J. Strickler, S.J. Lynch, D.K. Lee, R. Gruber, F. Troyon, Phys. Rev. Lett. 43 (1979), 1395.

4 Goedbloed, J.P., P.H. Sakanaka, Phys. Fluids 17 (1974), 908.

5 Gruber, R., F. Troyon, D. Berger, L.C. Bernard, S. Rousset, R. Schreiber, W. Kerner, W. Schneider, K.V. Roberts, Computer Phys. Commun. 21 (1981 a), 323.

6 Gruber, R., S. Semenzato, F. Troyon, T. Tsunematsu, W. Kerner, P. Merkel, W. Schneider, Computer Phys. Commun. 24 (1981 b), 363.

7 Kerner, W., P. Gautier, K, Lackner, W. Schneider, R. Gruber, F. Troyon, Nucl. Fusion 21 (1981), 1283.

8 Munro, J.K., L.A. Charlton, D.J. Strickler, W.A. Cooper, J.T. Hogon, D.W. Swain, Nucl. Fusion 22 (1982), 599.

9 Todd, A.M.M., J. Manickam, M. Okabayashi, M.S. Chance, R.C. Grimm, J.M. Greene, J.L. Johnson, Nucl. Fusion 19 (1979), 743.

FIGURE CAPTIONS

Fig. 1 : The stable region of INTOR at increasing values of the plasma current I. The parameters are R/a = 4, E = 1.6, γ = 0.3. M = Mercier limit on axis, B = ballooning limit. The curve labeled 10^{-4} is the n = 1 free-boundary σ-stability limit.

Fig. 2 : Profiles of the pressure p, safety factor q and current density j for 3 INTOR equilibria marginally stable to n = 1. I = 5.9 MA. The pressure is normalized to the magnetic pressure on axis. The scale of j is arbitrary. The radial coordinate R is normalized to 1 at the magnetic axis.

Fig. 3 : Unstable global n = 1 mode. The singular surfaces q = 2, 3 and 4 are visible because of the peaked shear velocity on them. q_0 = 1.35, I = 5.9 MA, β = 3 %.

Fig. 4 : Dependence of the free-boundary σ-stability limit as function of n.

Fig. 5 : Dependence of the maximum β on the plasma current I for INTOR and INTOR-like plasmas. The straight line is a fit through the INTOR values only.

Fig. 6 : Stable INTOR equilibrium with the highest beta.

Fig. 7 : The free-boundary and rigid boundary stability limits of JET extended performance. Stability is below and to the right of each curve.

Fig. 8 : Dependence of β limit on I for JET.

Fig. 9 : Profiles of the fully stable JET equilibrium with I = 9.6 MA and β = 5.5 %.

Fig. 10 : Dependence of the limiting βA given by the n = 1 free boundary mode on normalized current $I_N = \mu_0 IA^2/T_S$.

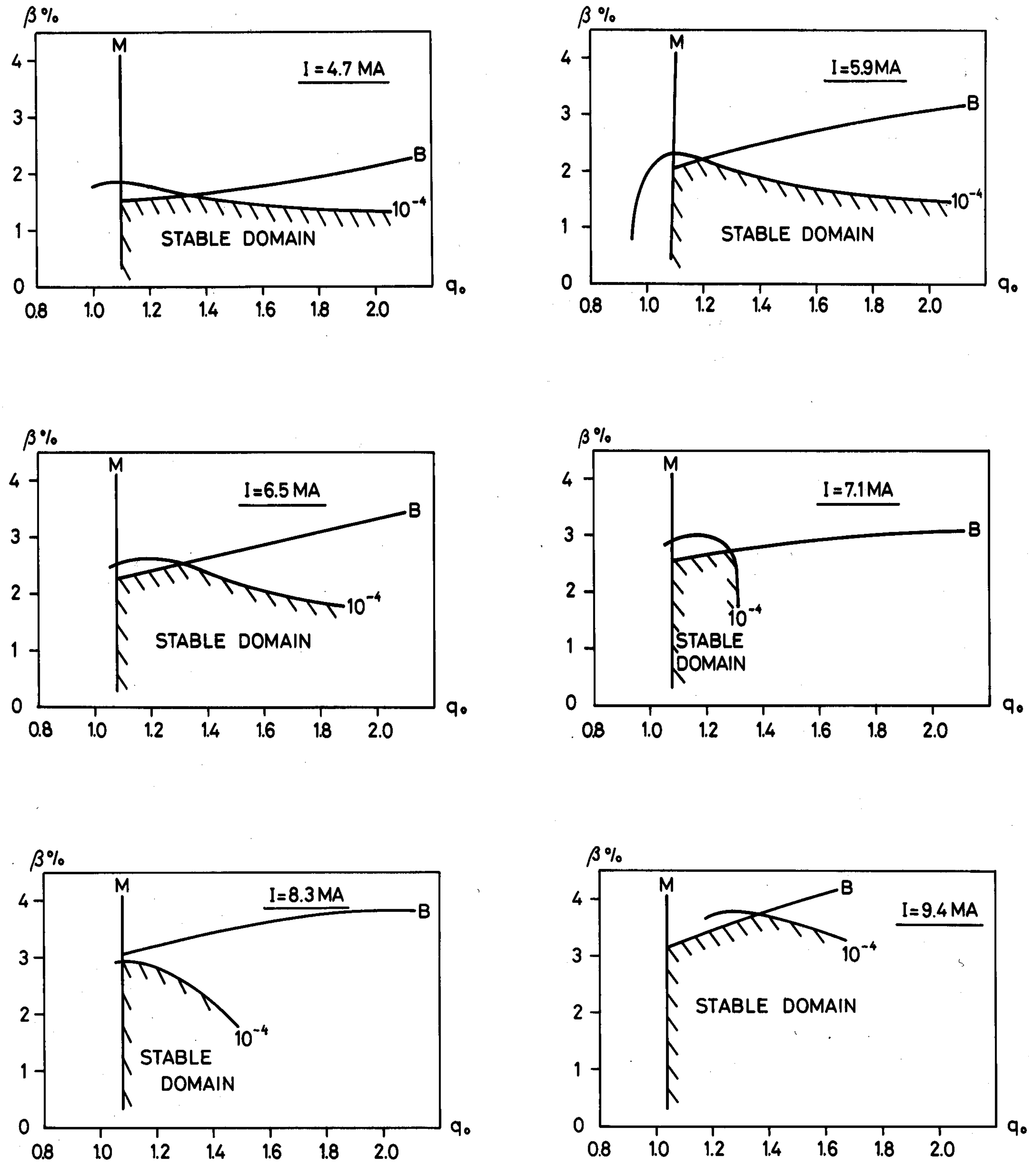
β %
M
I = 4.7 MA
B
10^-4
STABLE DOMAIN
q₀
I = 5.9 MA
I = 6.5 MA
I = 7.1 MA
I = 8.3 MA
I = 9.4 MA
0.8
1.0
1.2
1.4
1.6
1.8
2.0

Fig. 1

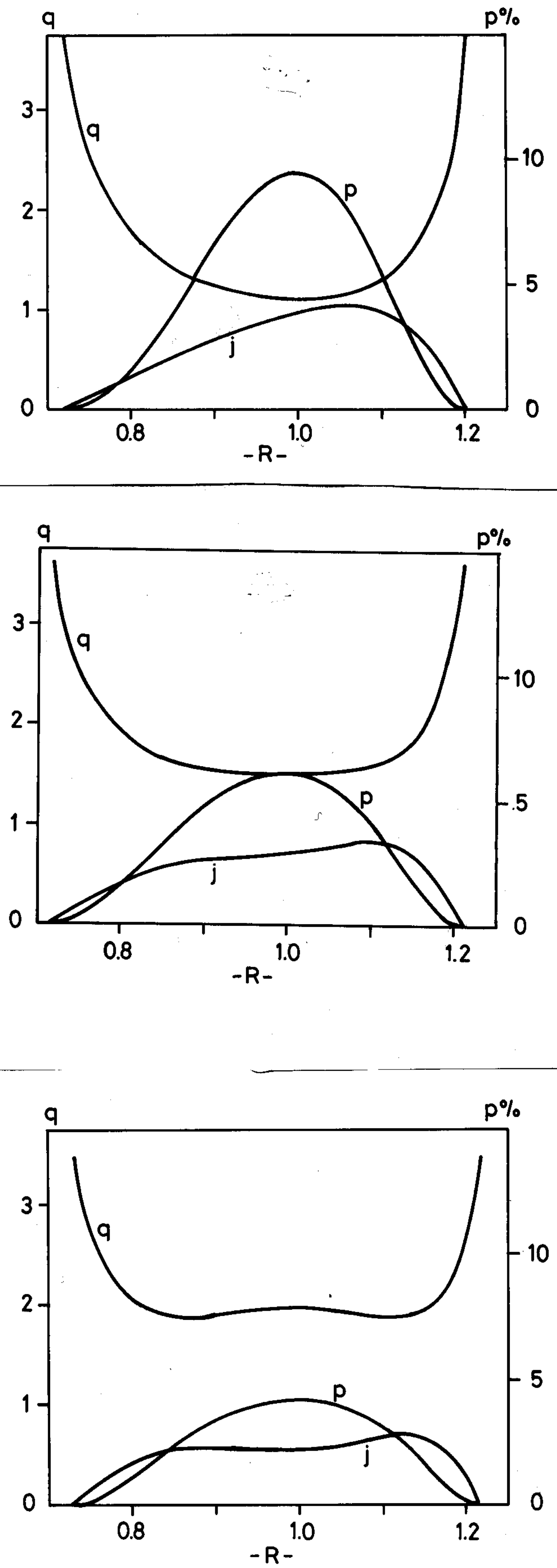
q
p%
3
2
1
0
10
5
0
0.8
1.0
1.2
-R-
q
p
j
q
p%
3
2
1
0
10
.5
0
0.8
1.0
1.2
-R-
q
p
j
q
p%
3
2
1
0
10
5
0
0.8
1.0
1.2
-R-
q
p
j

Fig. 2

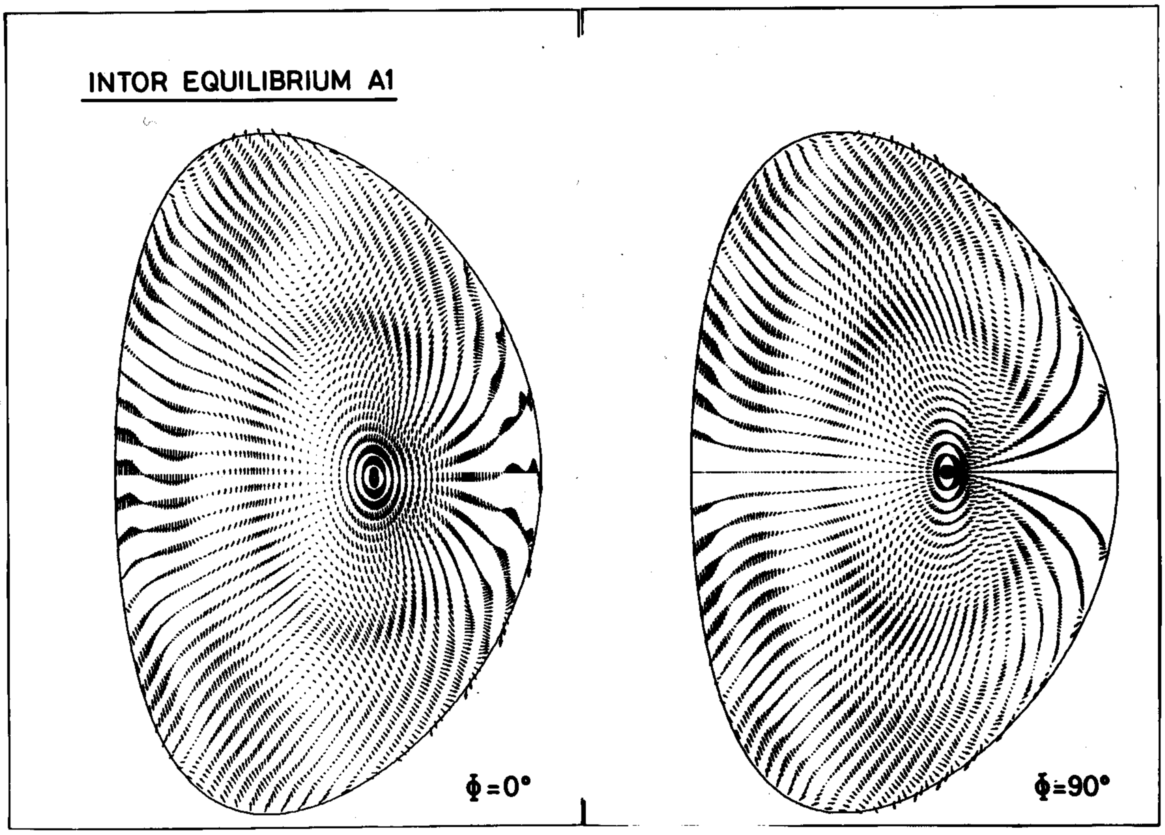

Fig. 3

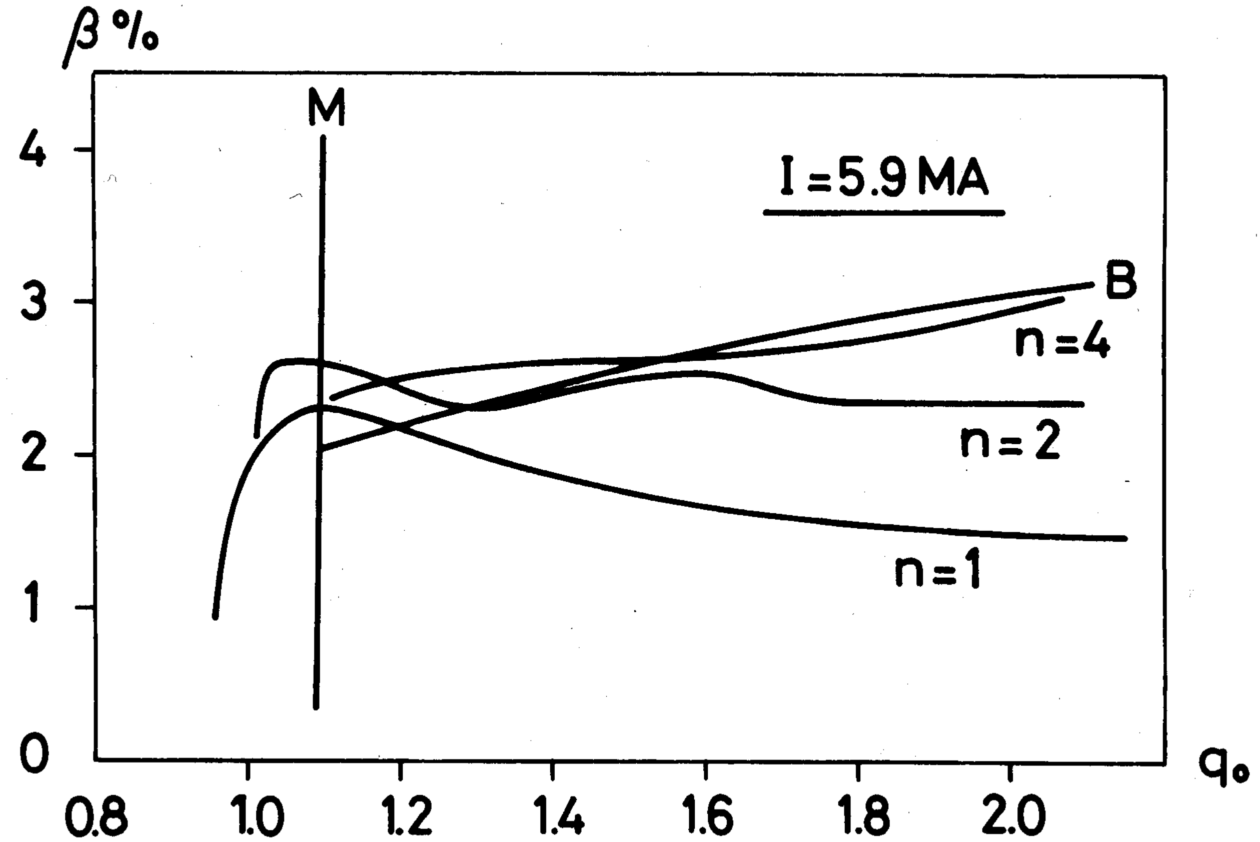

Fig. 4

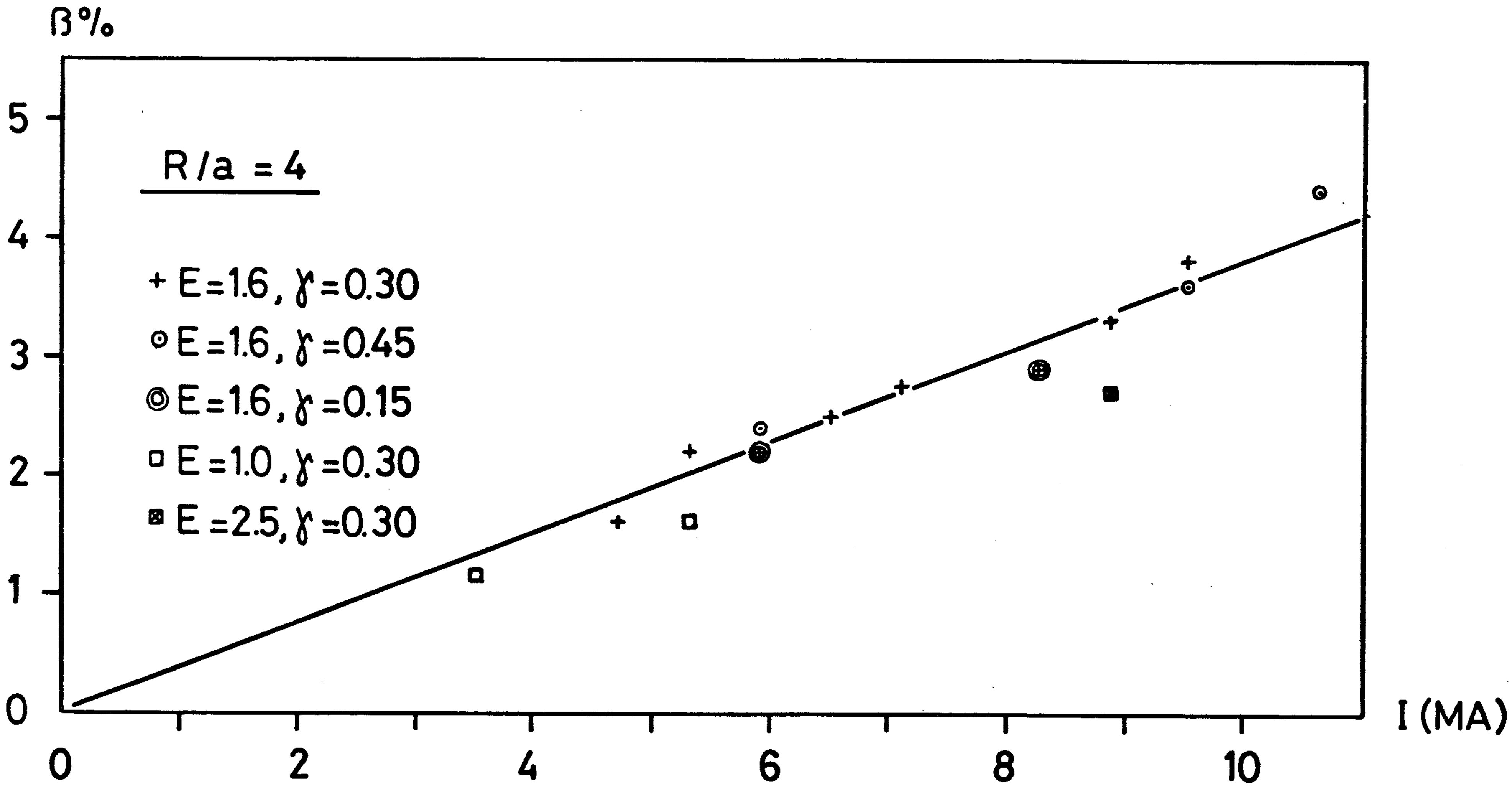
ß%
5
4
3
2
1
0
R/a = 4
+ E=1.6, γ=0.30
⊙ E=1.6, γ=0.45
◎ E=1.6, γ=0.15
□ E=1.0, γ=0.30
⊠ E=2.5, γ=0.30
0
2
4
6
8
10
I (MA)

Fig. 5

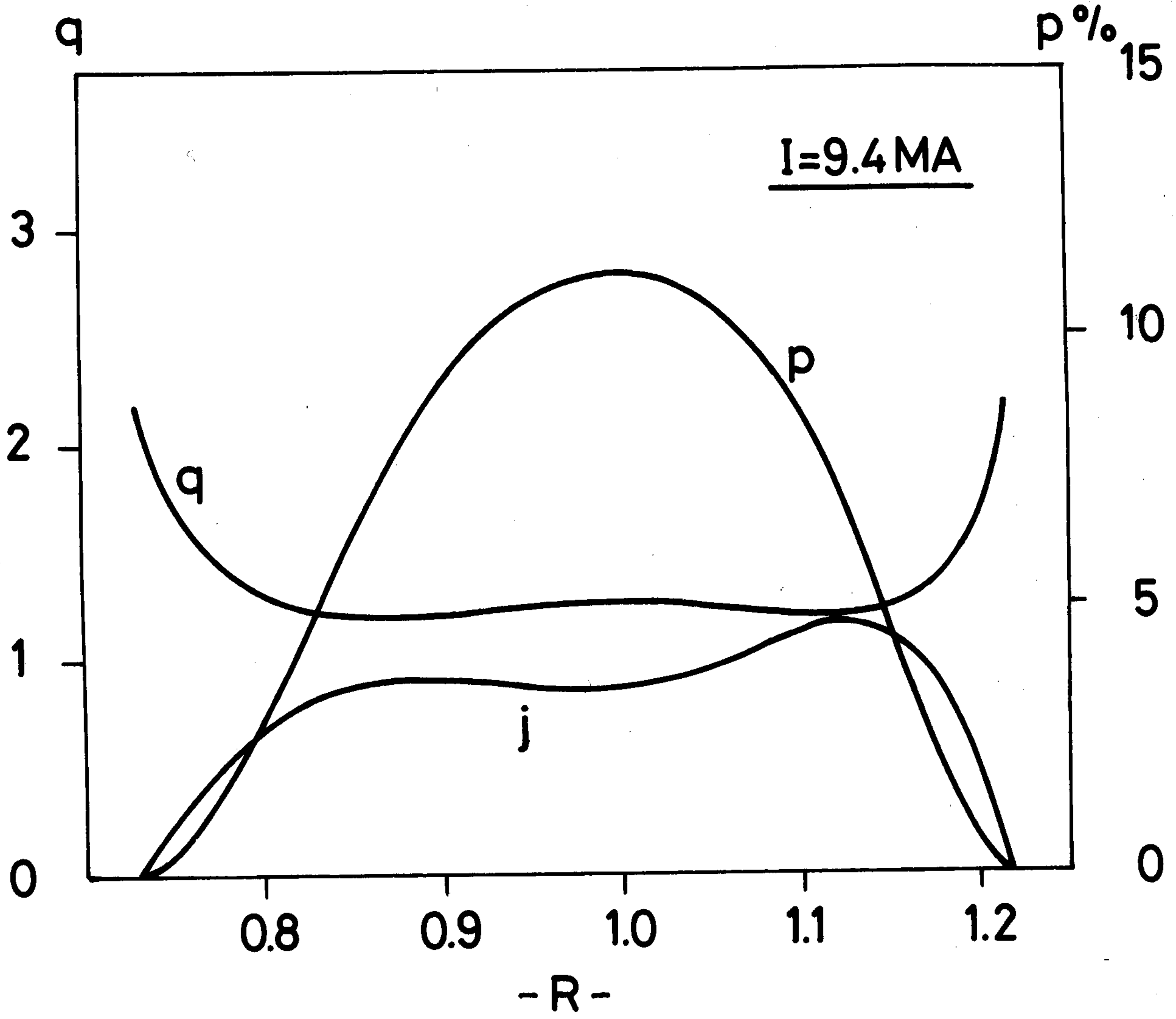

Fig. 6

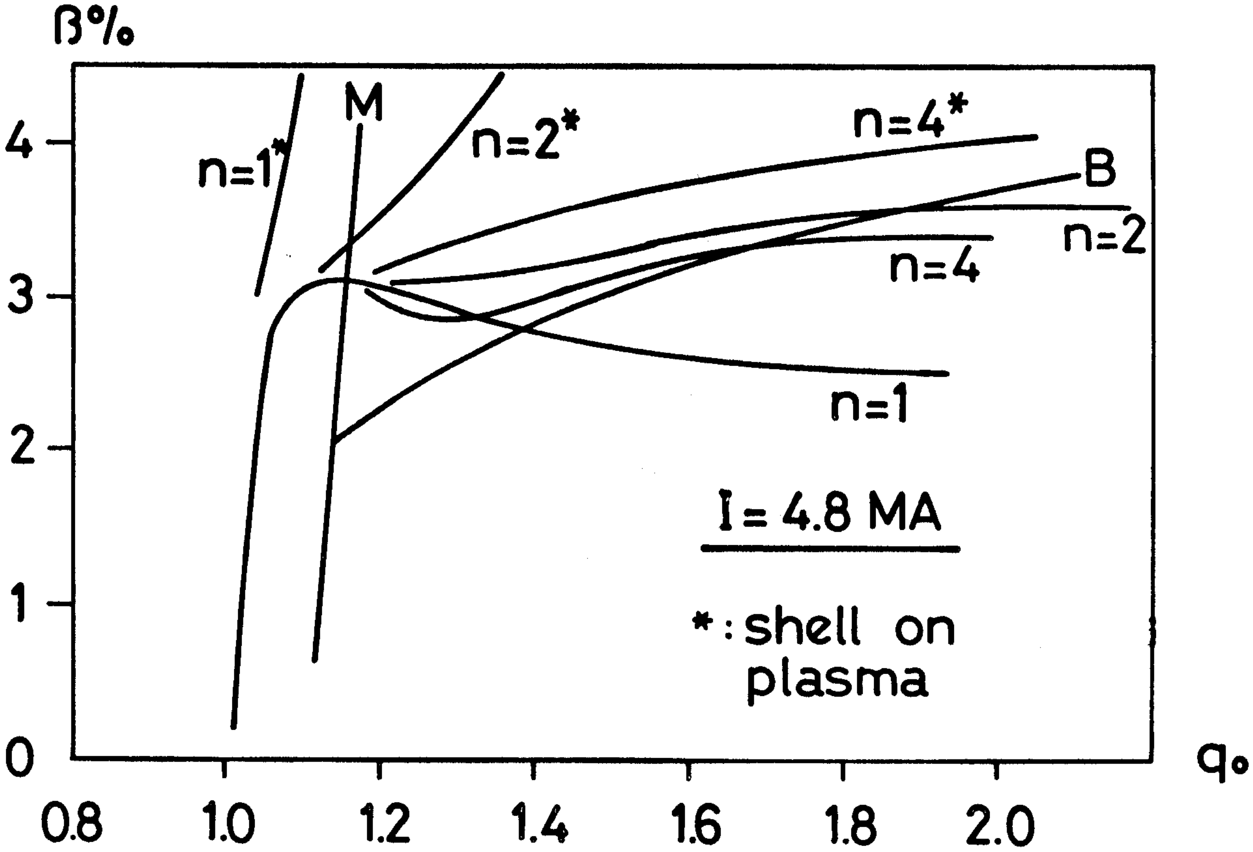

ß%
4
3
2
1
0
0.8
1.0
1.2
1.4
1.6
1.8
2.0
q₀
n=1*
M
n=2*
n=4*
B
n=2
n=4
n=1
I= 4.8 MA
*: shell on plasma

Fig. 7

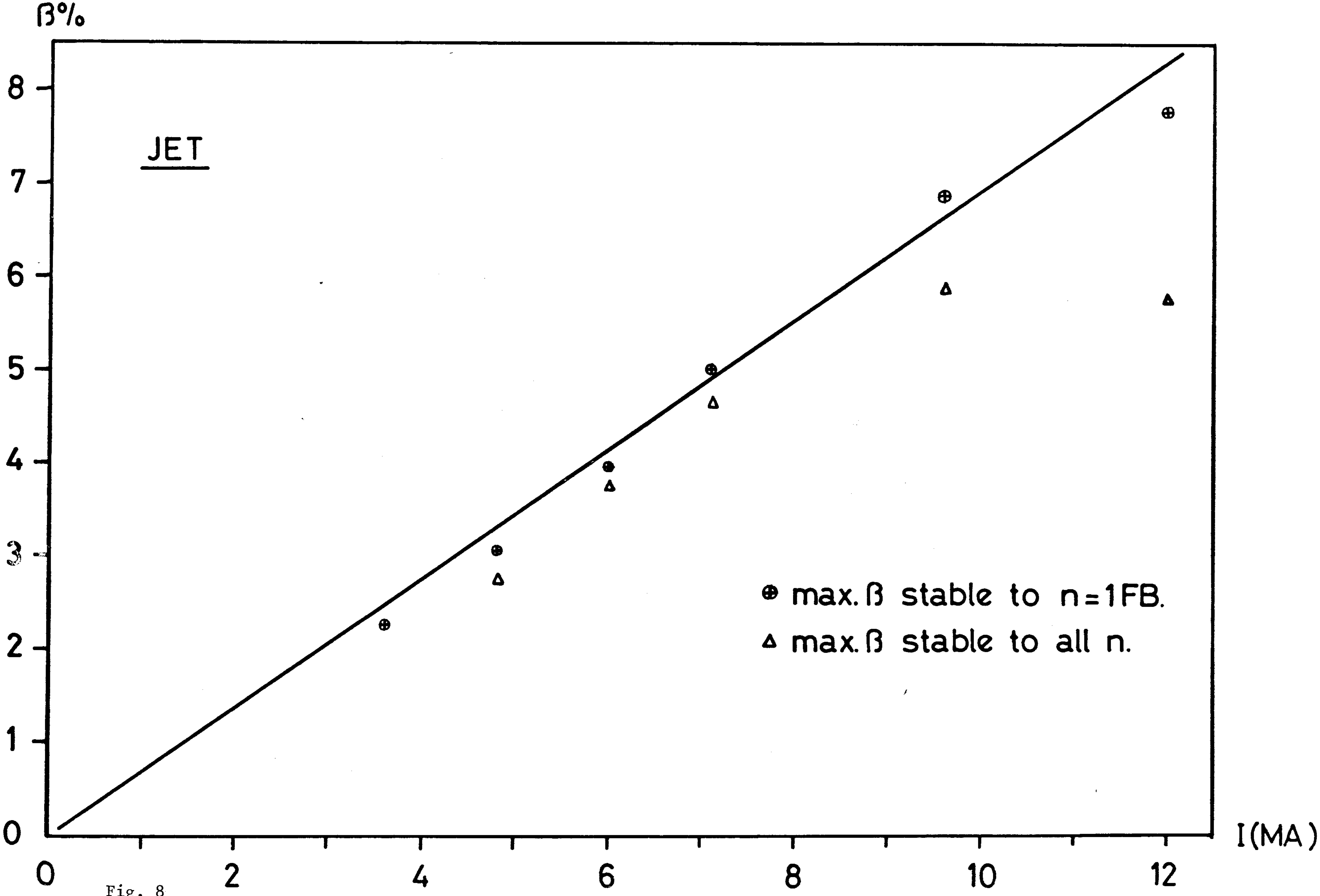
β%
JET
8
7
6
5
4
3
2
1
0
0
2
4
6
8
10
12
I(MA)
⊕ max.β stable to n=1FB.
△ max.β stable to all n.

Fig. 8

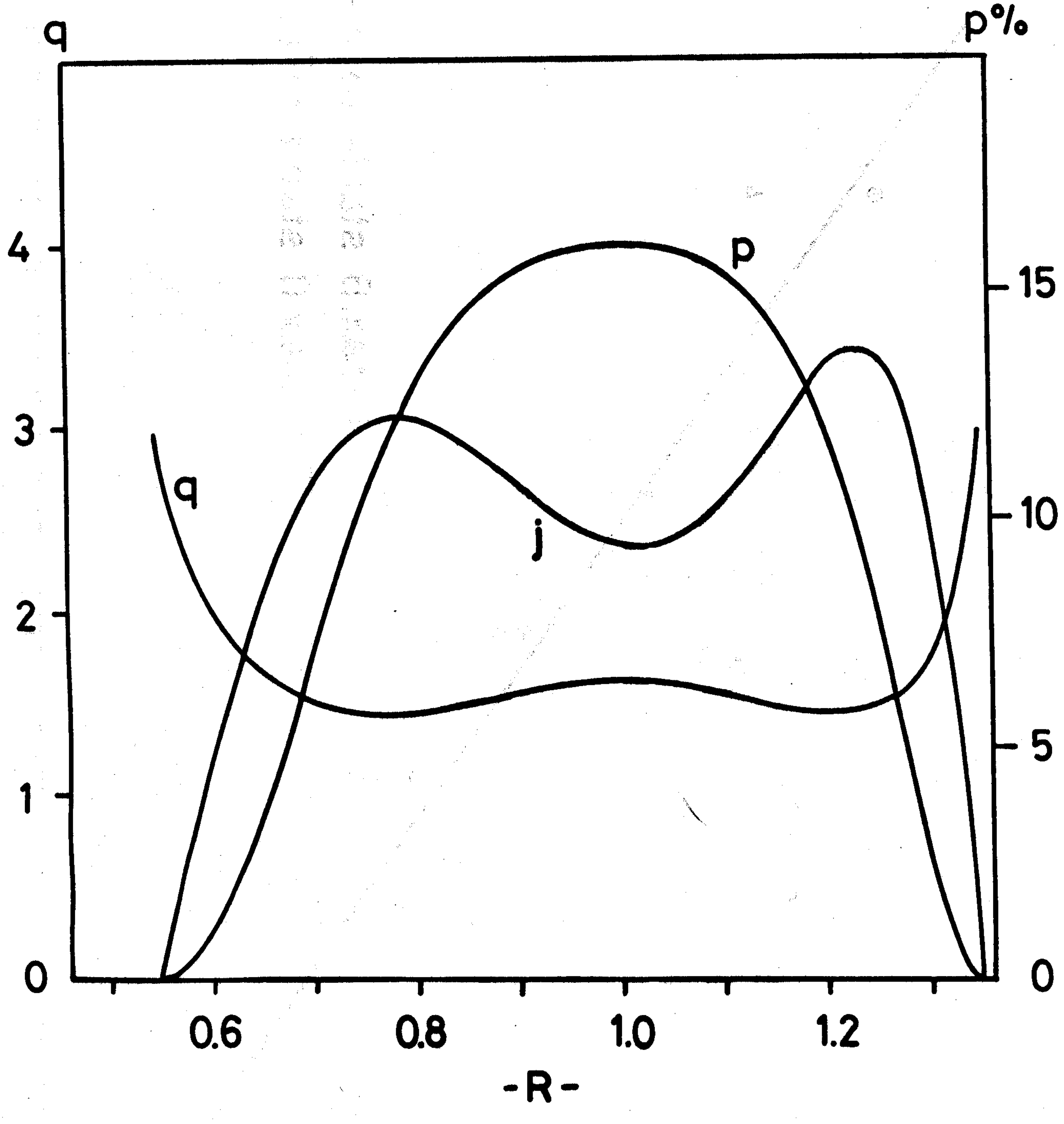

Fig. 9

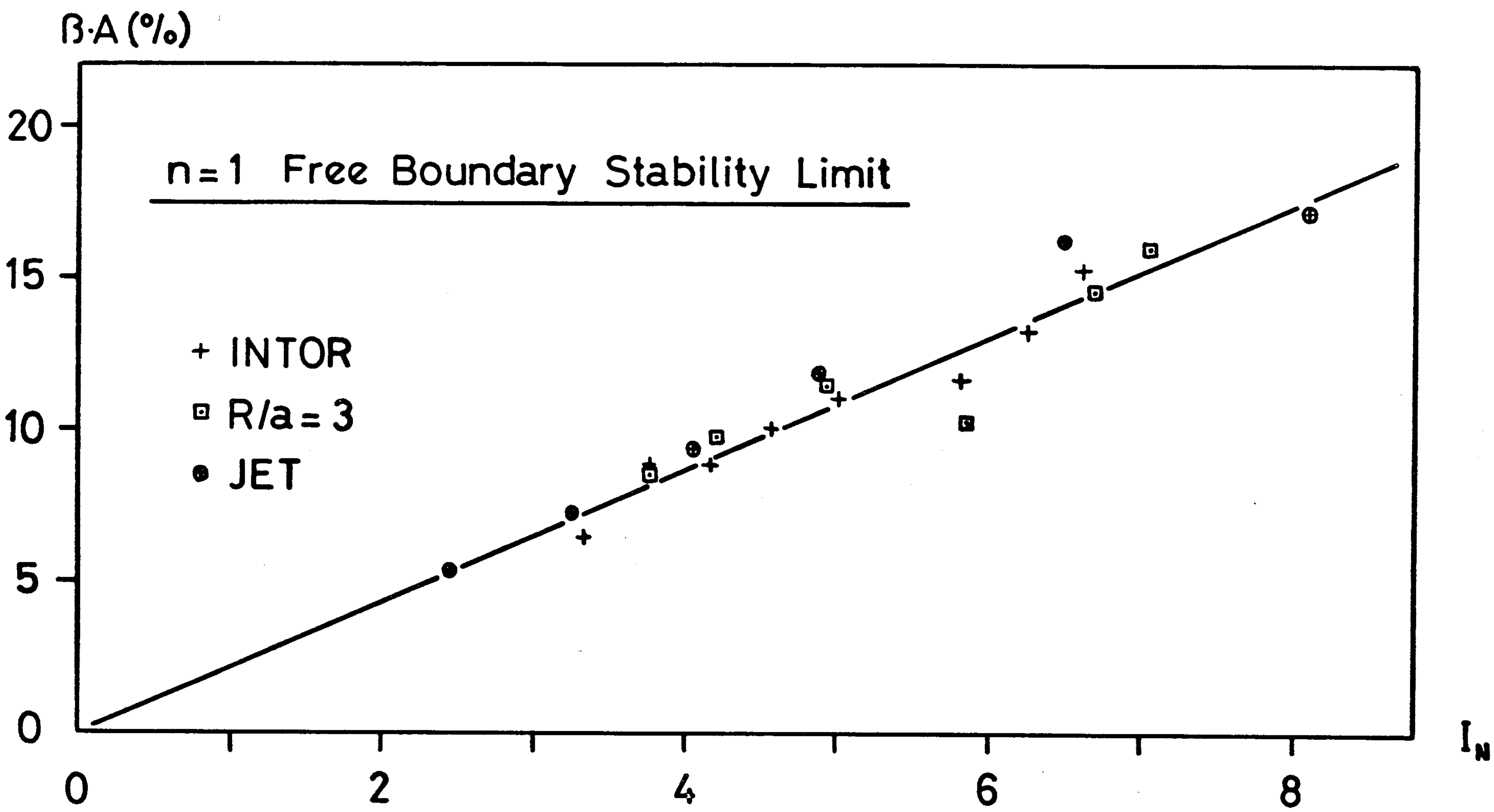
β·A (%)
n = 1 Free Boundary Stability Limit
+ INTOR
R/a = 3
JET
20
15
10
5
0
0
2
4
6
8
I_N

Fig. 10